Properties of n-type SnO_2 semiconductor prepared by spray ultrasonic technique for photovoltaic applications

H. Bendjedidi[1, †], A. Attaf[1], H. Saidi[1], M. S. Aida[2], S. Semmari[1], A. Bouhdjar[1], and Y. Benkhetta[1]

[1]Laboratoire de Physique des Couches Minces et Applications, Université de Biskra, BP 145 RP, 07000 Biskra, Algérie
[2]Laboratoire des Couches minces et Interfaces, Université Mentouri, 25000 Constantine, Algérie

Abstract: Transparent conducting n-type SnO_2 semiconductor films were fabricated by employing an inexpensive, simplified spray ultrasonic technique using an ultrasonic generator at deferent substrate temperatures (300, 350, 400, 450 and 500 ℃). The structural studies reveal that the SnO_2 films are polycrystalline at 350, 400, 450, 500 ℃ with preferential orientation along the (200) and (101) planes, and amorphous at 300 ℃. The crystallite size of the films was found to be in the range of 20.9–72.2 nm. The optical transmittance in the visible range and the optical band gap are 80% and 3.9 eV respectively. The films thicknesses were varied between 466 and 1840 nm. The resistivity was found between 1.6 and 4×10^{-2} Ω·cm. This simplified ultrasonic spray technique may be considered as a promising alternative to a conventional spray for the massive production of economic SnO_2 films for solar cells, sensors and opto-electronic applications.

Key words: tin oxide; thin films; spray ultrasonic; structural properties; optical properties
DOI: 10.1088/1674-4926/36/12/123002 **EEACC:** 2520

1. Introduction

Metal oxide semiconductors such as SnO_2, In_2O_3, CdO and ZnO have been used in the opto-electronic devices mostly for flat panel displays, photovoltaic devices, gas sensors and heat reflecting mirrors because of their suitable band gaps of 2.8–4.2 eV, n-type conductivity and other useful characteristics[1]. Tin oxide thin films are transparent and conductive, and are particularly useful when good transparency in the visible range and good electrical conductivity are simultaneously required[2]. SnO_2 films have high chemical stability and physical strength. SnO_2 films can also be used in energy conversion systems. This material could find application in semiconductor electrodes for hydrogen based photo-electrochemical conversion and solar cells. SnO_2 thin film can be prepared by a number of methods, such as CVD[3, 4], sputtering[5, 6], spray pyrolysis[7, 8], plasma and sol–gel methods[9], each of which had advantages and disadvantages. The preparation of SnO_2 films has been well established by a spray ultrasonic technique. This technique is simple, inexpensive and permits easy deposition in the atmospheric condition. The optical and structural properties of spray deposited SnO_2 films have also been well studied[10, 11], due to the greater interest of SnO_2 thin films. The main accomplishment of this work is to characterize the SnO_2 films (structural, optical and electrical characterisation) deposited by the spray ultrasonic process, and the film's properties dependence from the deposition conditions and the substrate temperatures. This is an important parameter for understanding the nature of thin film and its uses for required applications.

2. Experimental procedure

Tin oxide thin films were prepared by spraying an alcoholic solution that contains Tin Chloride dehydrate $SnCl_2$-$2H_2O$ and CH_4O onto glass substrates with deferent temperatures using ultrasonic spray process. Substrates were cleaned and degreased successively with Acetone, propanol, and distilled water. The films were deposited with a precursor molarity of 0.1 mol/L, and we have varied the temperature from 300 to 500 ℃ in atmospheric pressure. The films were characterized by means of structural, optical and electrical techniques. The film's thickness was calculated from the interference fringes obtained from transmittance spectra by the UV–VIS–NIR transmittance. The X-ray diffraction studies were carried out using a D8 ADVANCED BRUKER diffractometer with a copper anode having a wavelength $\lambda = 1.5418$ Å; the crystallite sizes were estimated to study the effect of the temperature. The UV–VIS–NIR transmittance measurements were performed by using a PerkinElmer LAMBDA1050 UV/VIS/NIR spectrometer in the spectral range 300–1500 nm.

3. Results and discussion

3.1. Structural properties

The X-ray diffraction patterns for SnO_2 films deposited at 300, 350, 400, 450 and 500 ℃ are shown in Figure 2. It can be found that films deposited at 300 ℃ were nearly amorphous whereas for higher temperatures, the amorphous background was diminished and diffraction peak (110) of standard SnO_2 powder revealed for all samples as mentioned by other researchers[12–15]. While the films deposited at higher temperatures exhibit five peaks. It is evident that the films deposited at 350, 400, 450 and 500 ℃ are polycrystalline in nature. In all films the half width of the Bragg peak decreases and displays gradual change in the preferred orientation from (101) to (200)

† Corresponding author. Email: h.bendjedidi@gmail.com
Received 19 April 2014, revised manuscript received 7 July 2014

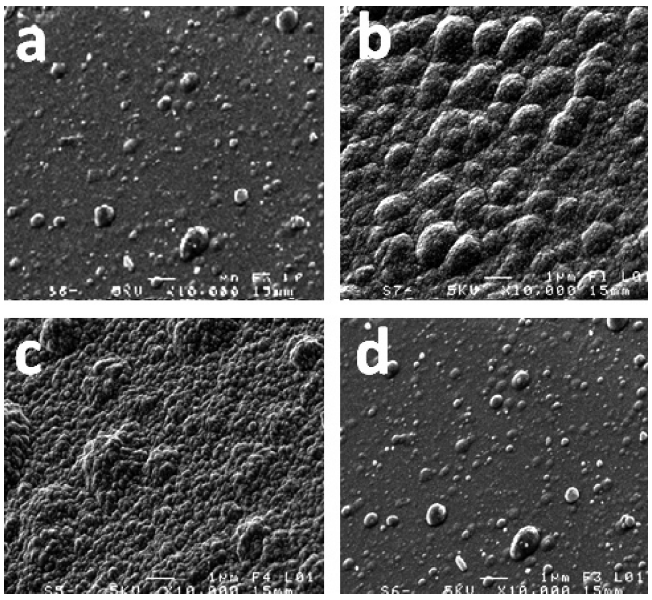

Figure 1. SEM images of SnO_2 thin films deposited on glass substrates at different temperatures. (a) 300 ℃. (b) 350 ℃. (c) 400 ℃. (d) 450 ℃.

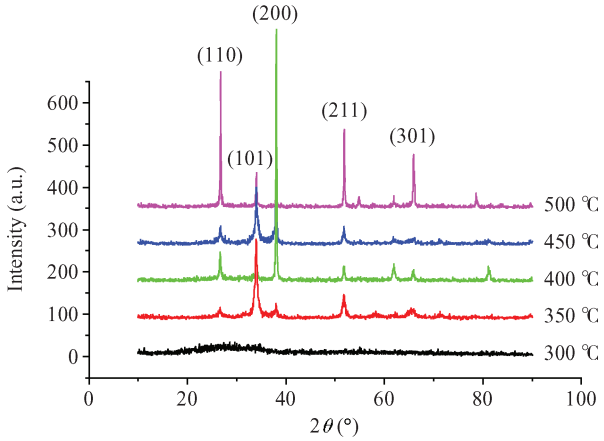

Figure 2. (Color online) X-ray diffraction pattern of SnO_2 films at various substrate temperatures.

plane with an increase in the substrate temperature from 350 to 500 ℃[16].

In order to determine the variation of the crystallite size with increasing substrate temperatures, the size of the crystallites oriented along the (101) plane is calculated using Scherrer's formula[17, 18]

$$D = \frac{0.94\lambda}{\Delta\theta_{hkl}\cos\theta_{hkl}}, \tag{1}$$

where D is the size of crystallite, $\Delta\theta_{hkl}$ the broadening of diffraction line measured at half its maximum intensity in radians and λ is the wavelength of X-rays (1.54 Å). The calculated values of crystallite size are given in Figure 3. It can be seen that the substrate's temperatures had an effective influence on the crystallite size, which increased from 21.9 to 72.2 nm. The growth in crystallite size is due to the fact by the increasing substrate's temperatures, which at higher than 300 ℃ during deposition was relatively high and enough to provide sufficient thermal energy for recrystallization. Hence, the crystallization process improved and the smaller crystallites agglomerated with increasing substrate temperature to cause a change in crystallite size distribution towards larger crystallites. This result is in agreement with those of other researchers[19, 20].

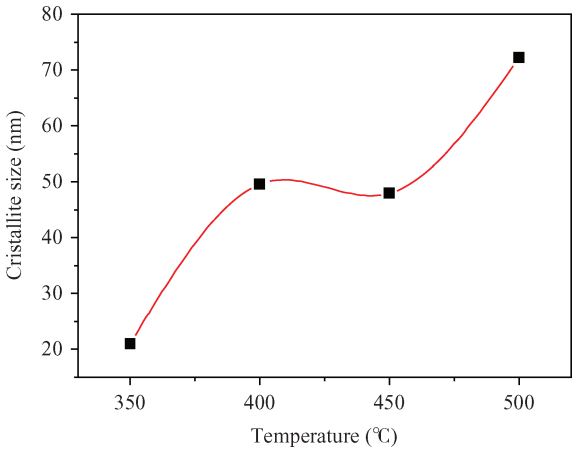

Figure 3. Dependence of the crystallite size versus substrate temperatures.

3.2. Optical properties

The optical transmission spectrum for SnO_2 films deposited at 300, 350, 400, 450 and 500 ℃ are shown in Figure 4, which shows the variation of transmittance with respect to the wavelength of SnO_2 thin films deposited at various substrate temperatures. The average transmission in the visible region has been found to be ranging from 60% to 80% depending upon the substrate temperature. An increase in transmission is observed with an increase in temperature. At lower temperatures, at 350 ℃, a relatively lower transmission is due to the formation of milky films and that is because of incomplete decomposition of the sprayed droplets. In general, in the visible region of the spectrum, the transmission is high (high enough to observe interference fringes). It is due to the fact that the reflectivity is low and there is no (or less) absorption due to the transfer of electrons from the valence band to the conduction band owing to optical interference effects, so it is possible to maximize the transmission of thin film at a particular region of wavelengths[21].

We have used the pattern of transmission in the transparent region with successive minima and maxima to evaluate the thickness of the SnO_2 films. The thickness d of the films can be calculated from the following equations[22]:

$$N_{1,2} = 2S\frac{T_M - T_m}{T_M T_m} + \frac{S^2+1}{2}, \tag{2}$$

$$n_{1,2} = \left[N_{1,2} + (N_{1,2}^2 - S^2)^{1/2}\right]^{1/2}, \tag{3}$$

$$d = \frac{\lambda_1\lambda_2}{2(n_1\lambda_2 - n_2\lambda_1)}, \tag{4}$$

where d is the film's thickness, T_M and T_m are maxima and minima transmittance respectively, and n, s are the film and glass refractive indices respectively.

The film's optical band gap has been determined on the basis of UV–VIS transmission measurements. The band gap (E_g)

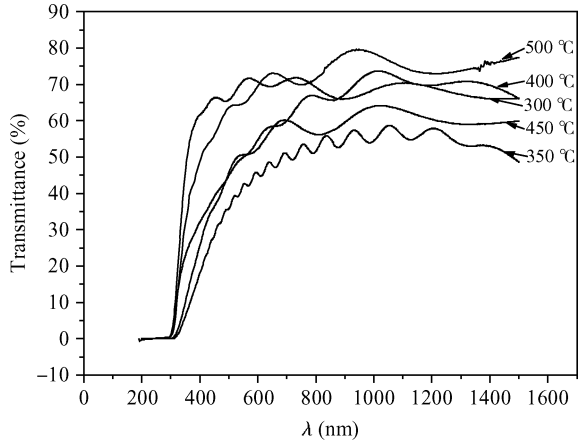

Figure 4. The transmittance spectra of SnO_2 films at various substrate temperatures.

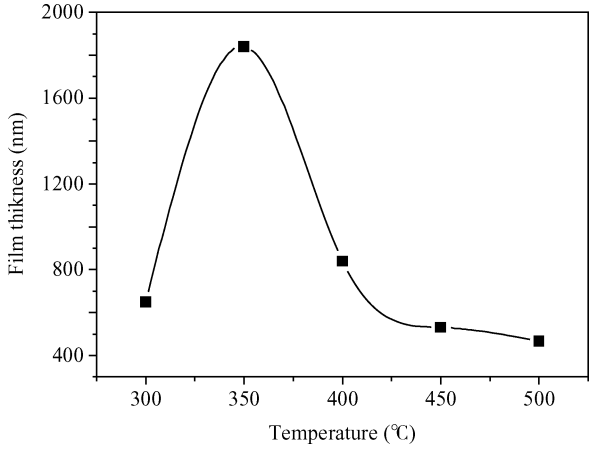

Figure 5. Dependence of thickness versus the substrate temperatures.

is determined by extrapolating the straight line portion of the plot to the energy axis. The intercept on the energy axis gives the value of band gap energy E_g for all the samples. The obtained optical band gap values lie in the range 3.92–3.98 eV. In Figure 5 we have reported the variation of film thickness as a function of temperature. It shows that the film thickness decreases almost linearly with substrate temperature in the range 350–500 ℃, owing to the increased evaporation rate of the initial product with a rise in substrate temperature leading to the diminished mass transport towards the substrates[23]. At lower substrate temperatures 350–400 ℃, the temperature may not be sufficient to decompose the sprayed droplets of Sn^{2+} from the solution and this therefore, results in an increase of film thickness[24].

The variation of band gap E_g as a function of substrate temperature is shown in Figure 6.

The obtained energy gap values are in good agreement with other literature reports[25, 26]. It is found that the band gap energy decreases with increasing substrate temperature in the range 300–350 ℃. The values of band gap lie in the range of 3.92–3.98 eV taking into account the experimental errors; these values of band gap indicate that the SnO_2 films had a direct band gap energy[27]. This result can be attributed to the decrease of grain boundaries as scattering centers. In fact, the increase of substrate temperature improves the crystallinity and

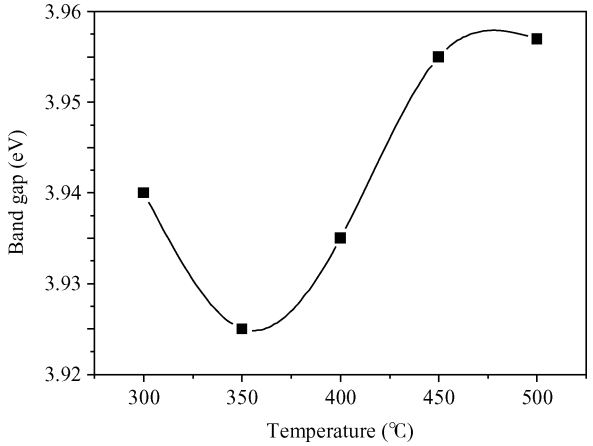

Figure 6. Dependence of the Band Gap versus the substrate temperatures.

increases the average crystallite size, which results in decreasing grain boundaries; therefore, the band gap energy decreases. At high temperatures in the range 350–500 ℃, the increment of band gap energy with substrate temperature may be attributed to the partial filling of the conduction band of tin oxide, resulting in a blocking of the lowest states. This widening of the optical band gap is termed as a Burstein-Moss shift[28]. This shift is given by the relation:

$$E_g = E_{g0} + \Delta E_g^{BM}, \tag{5}$$

where E_{g0} is the intrinsic band gap and ΔE_g^{BM} is the Burstein-Moss shift. This shift is related to the carrier density as:

$$\Delta E_g^{BM} = \frac{\pi^2 h^2}{2m^*}\left(\frac{3N}{\pi}\right)^{\frac{2}{3}}, \tag{6}$$

where m^* is the reduced effective mass, h is the Plank's constant and N is the carrier concentration.

3.3. Electrical properties

Electrical resistivity measurements have been carried out using the two-probe method. The variation of electrical resistivity of the SnO_2 films as a function of temperature is shown in Figure 7. It is observed that the resistivity of the films in the first decreases slowly with temperature in the range of 350–400 ℃ and rapidly between 400 and 450 ℃. In fact, two competing processes of thermal excitation of electrons and oxygen adsorption occur simultaneously. The gradual reduction in film resistivity in the temperature range 350–400 ℃ is because the thermal excitation of electrons dominates over the oxygen adsorption process, while the sharp decrease in the film resistivity with temperature in the range 400–450 ℃ may be the result of improved adsorption of atmospheric oxygen at this range of temperatures. In fact this may be attributed to the adsorption of atmospheric oxygen on the film surface. In temperatures up to 450 ℃, the resistivity increases rapidly; it could be due to the grain boundaries effect that plays the role of traps for the electrons and consequently the film resistivity is increased. The variation of the resistivity can be also explained by the effect of films thickness. As reported in Figure 5, the variation of the latter is opposite to the resistivity.

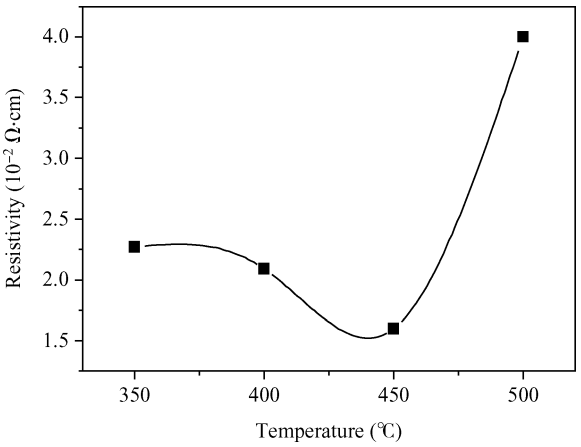

Figure 7. Resistivity as a function of substrate temperature.

4. Conclusion

Highly transparent films of Tin oxide have been prepared by an ultrasonic spray CVD process. Films deposited at a temperature higher than 350 ℃ were identified as polycrystalline tin oxide films. The increase of temperature in the range of 350–500 ℃ improves the film's crystallinity and enhanced the crystallite size. The transmission in the visible and infrared regions of deposited films was found to be weakly affected by the temperature deposition between 300 and 500 ℃, in which range the film's transmittance exceeds 80%. The optical band gap values ranges between 3.92–3.98 eV for films deposited at different temperatures. The resistivity was found in the range of 0.016 to 0.04 Ω·cm. These films were suitable for low cost opto-electronic applications such as transparent conductive electrode, flat panel display and window filter in photovoltaic devices.

References

[1] Yang C H, Lee S C, Chen S C. The effect of annealing treatment on microstructure and properties of indium tin oxides films. Mater Sci Eng, 2006, B 129: 154

[2] Ayeshamariam A, Sanjeeviraja C, Samy R P. Synthesis, structural and optical characterizations of SnO_2 nanoparticles. Journal of Photonics and Spintronics, 2013, 2(2): 4

[3] Khanaa V, Mohanta K. Synthesis and structural characterization of SnO_2 thin films prepared by spray pyrolysis technique. International Journal of Advanced Research, 2013, 1(7): 666

[4] Liang Y, Zheng H, Fang B. Synthesis and characterization of SnO with controlled flower like microstructures. Mater Lett, 2013, 108: 235

[5] Benouisa C E, Benhalilibaa M, Yakuphanoglub F, et al. Physical properties of ultrasonic sprayed nanosized indium doped SnO_2 films. Synthetic Metals, 2011, 161: 1509

[6] Jäger T, Bissig B, Döbeli M, et al. Thin films of SnO_2:F by reactive magnetron sputtering with rapid thermal post-annealing. Thin Solid Films, 2014, 553: 21

[7] Rubinger C P L, Cunha A F, Vinagre F, et al. Microwave shielding of fluorine-doped tin oxide film obtained by spray pyrolysis studied by electrical characterization. J Appl Phys, 2009, 105: 074502

[8] Barıþ B. AC conductivity and dielectric spectroscopy studies on tin oxide thin films formed by spray deposition technique. Physica B, 2014, 438: 53

[9] Lehrzki N, Aida M S, Abed S, et al. ZnO thin films deposition by spray pyrolysis: influence of precursor solution properties. Current Applied Physics, 2012, 12(5): 1283

[10] Rani S, Roy S C, Karar N, et al. Structure, microstructure and photoluminescence properties of Fe doped SnO_2 thin films. Solid State Commun, 2007, 141: 214

[11] Bhardwaj N, Kuriakose S, Mohapatra S. Structural and optical properties of SnO_2 nanotowers and interconnected nanowires prepared by carbothermal reduction method. Journal of Alloys and Compounds, 2014, 592: 238

[12] Ren Y, Zhao G, Chen Y. Fabrication of textured SnO_2:F thin films by spray pyrolysis. Appl Surf Sci, 2011, 258: 914

[13] Sefardjella H, Boudjema B, Kabir A, et al. Characterization of SnO_2 obtained from the thermal oxidation of vacuum evaporated Sn thin films. J Phys Chem Solids, 2013, 74: 1686

[14] Babar A R, Shinde S S, Moholkarb A V, et al. Electrical and dielectric properties of co-precipitated nanocrystalline tin oxide. Journal of Alloys and Compounds, 2010, 505: 743

[15] Babar A R, Shinde S S, Moholkarb A V, et al. Structural and optoelectronic properties of antimony incorporate tin oxide thin films. Journal of Alloys and Compounds, 2010, 505: 416

[16] Patil P S, Sadale S B, Mujawar S H, et al. Synthesis of electrochromic tin oxide thin films with faster response by spray pyrolysis. Appl Surf Sci, 2007, 253: 8560

[17] Ynineb F, Hafdallah A, Aida M S, et al. Influence of Sn content on properties of ZnO:SnO_2 thin films deposited by ultrasonic spray pyrolysis. Materials Science in Semiconductor Processing, 2013, 16: 2021

[18] Yang M R, Chu S Y, Chang R C. Synthesis and study of the SnO_2 nanowires growth. Sensors and Actuators, 2007, B122: 269

[19] Kasar R R, Deshpande N G, Gudage Y G, et al. Studies and correlation among the structural, optical and electrical parameters of spray-deposited tin oxide (SnO_2) thin films with different substrate temperatures. Physica B, 2008, 403: 3724

[20] Patil G, Kajale D, Chavan D, et al. Synthesis, characterization and gas sensing performance of SnO_2 thin films prepared by spray pyrolysis. Bull Mater Sci, 2011, 34(1): 1

[21] Miao D, Zhao Q, Wu S, et al. Effect of substrate temperature on the crystal growth orientation of SnO_2:F thin films. Journal of Non-Crystalline Solids, 2010, 356: 2557

[22] Lin Lingyan, Yu Jinling, Cheng Shuying, et al. Influence of Ag and Sn incorporation in In_2S_3 thin films. Chin Phys B, 2015, 24(7): 078103

[23] Chopra K L, Major S, Pandya D K. Transparent conductors—a status review. Thin Solid Films, 1983, 102: 15

[24] Ian Y Y. Effects of the pre-annealing temperature on structural and optical properties of sol–gel deposited aluminum doped zinc oxide. Ceramics International, 2014, 40: 11941

[25] Benamar E, Rami M, Messaoudi C, et al. Structural, optical and electrical properties of indium tin oxide thin films prepared by spray pyrolysis. Solar Energy Materials and Solar Cells, 1999, 56: 125

[26] Wang C. Enhanced photocatalytic performance of nanosized coupled ZnO/SnO_2 photocatalysts for methyl orange degradation. Journal of Photochemistry and Photobiology, 2004, 168: 47

[27] Raghupathi P S, George J, Menon C S. Effect of substrate temperature on the electrical and optical properties of reactively evaporated tin oxide thin films. Indian Journal of Pure and Appl Phys, 2005, 43: 622

[28] Tatar D, Turgut G, Düzgün B. Effect of substrate temperature on the crystal growth orientation and some physical properties of SnO_2:F thin films deposited by spray pyrolysis technique. Rom J Phys, 2013, 58: 143